Dielectric properties of spinel $Co_{3-x}Mn_xO_4$ (x = 0.1, 0.4, 0.7, and 1.0) ceramic compositions

P L Meena[1,*], K Sreenivas[2] & Ravi Kumar[3]

[1]Department of Physics, Deen Dayal Upadhyaya College (University of Delhi), Shivaji Marg, Karampura,
New Delhi 110 015, India

[2]Department of Physics andAstrophysics, University of Delhi, Delhi 110 007, India

[3]Beant College of Engineering and Technology, Gurdaspur, Punjab 143 521, India

*E-mail: plmeena@gmail.com, plmeena@ddu.du.ac.in

Cobalt manganese oxides $Co_{3-x}Mn_xO_4$ (x = 0.1, 0.4, 0.7, and 1.0) multi-ferroic ceramic were prepared by conventional solid state technique to understand the effect of Mn substitution at Co site on the structural and dielectric properties. Single phase polycrystalline with a linear increase in the lattice parameter 'a' was observed without any structural change in cubic crystal symmetry with Mn substitution. The effect of Mn substitution on the dielectric constant (ε') and loss tangent ($\tan\delta$) was measured over a wide temperature range (150-450 K) and frequency range (100-900 kHz).A very weak frequency dispersion and small temperature dependence was observed in ε' and $\tan\delta$ at low temperature, however, ε' and $\tan\delta$ display a strong frequency and temperature dependency at higher temperature.The ε'shows a ferroelectric like transition and shift to lower temperature with Mn incorporation.The behaviour of $\tan\delta$ shows dielectric relaxation and also shifts towards lower temperature with Mn incorporation. The ceramic compositions show universal dielectric response with temperature dependent exponent factor 's' and which fall in Jonscher's range.

Keywords: Dielectric properties, Ceramic, Jonscher's range

1 Introduction

Mixed spinel oxides form a special class of compounds and play an important role in variety of technological applications with interesting multi-disciplinary fields[1-6] and have been extensively investigated by introducing a variety of dopants[7-10]. The mixed spinel oxides with general formula AB_2O_4 (where A and B both are transition metal cations) can be considered as an interesting system due to their electronic, magnetic, optical and catalytic properties[11,12]. The compositional stoichiometry and the occupancy of the cations at tetrahedral A-site and octahedral B-site, some of the cobalt manganese $Co_{3-x}Mn_xO_4$ spinel phases seem to be likely for their multiferroic in which both ferromagnetic and ferroelectric properties can co-exist simultaneously[13,14]. In recent years, Co_3O_4 has also been identified as a magnetic semiconductor[15]and room temperature ferromagnetism in its nanostructures[16] and in one of our earlier reported paper[13] an interesting evidence through dielectric phase transition and magnetic properties has been noted in single phase Mn content Co_3O_4 indicating its multiferroic nature. Earlier studies on $Co_{3-x}Mn_xO_4$ (x = 0.1 to 1.0) have revealed

its ordered ferrimagnetic behaviour, and a phase transition from para-to ferrimagnetic[11] below 191 K. From the doping point of view, $CoCo_2O_4$ cubic spinel has lot of opportunity to doped various trivalent transition cations Al, Mn, Ni, Cr, Ti etc.) by replacing a fraction of Co^{3+} ions at octahedral site[11,17,18]. The motivation for the substitution of Mn^{3+} ions having a larger ionic radiuscompare to Co^{3+} ions is to look into the possibility of developing a new class of single phase multiferroic materials with the expectation that Mn can induce non-centro-symmetric charge ordering and consequent polarization.

In the present paper, we focus to engineer a class of materials by incorporation of Mn ion in the spinel structure of cobalt oxide. The structural and dielectric properties of $Co_{3-x}Mn_xO_4$ (x = 0.1, 0.4, 0.7, and 1.0) ceramic compositions prepared by solid-state reaction to identify the formation of single phase,effects on the lattice distortion and variation of dielectric properties, have been presented.

2 Experimental Details

Cobalt based spinel oxides $Co_{3-x}Mn_xO_4$ (x = 0.1, 0.4, 0.7 and 1.0) ceramic compositions were

synthesized by solid-state reaction method using high purity (> 99.97%) MnO and Co_3O_4 materials. The detailed preparation methods of these ceramic compositions were discussed elsewhere[14,19]. Room temperature powder X-ray diffraction (XRD) patterns were recorded using a Bruker AXS X-ray diffractometer with Cu K_α radiation in the 2θ range 20°-70°. For metal-insulator-metal configuration both faces of cylindrical discs were highly polished and coated with fine silver paste to serve as electrodes for dielectric measurement. The dielectric measurement of the ceramic compositions was carried out using Agilent (HP4192) precision LCR meter as a function of temperature in the range 150-450 K with temperature interval of 2 Kat fixed frequency using a special designed three terminal sample cell. The variation of temperature was controlled using a Lakeshore temperature controller with ± 0.05 K accuracy and the dielectric data was collected when the temperature was stable at each step.

3 Results and Discussion

Figure 1 shows the powder XRD patterns for $Co_{3-x}Mn_xO_4$ (CMO) with x = 0.1, 0.4, 0.7 and 1.0 ceramic compositions.The diffraction patterns show the formation of a single phase with cubic spinel structure and all the observable reflections could be indexed as shown in Fig. 1, and also found to be in agreement with earlier reported results[20]. The room temperature XRD data obtained on CMO ceramics were analyzed by Rietveld profile refinement method. Figure 2 shows the typical profile for the $Co_{0.3}Mn_{0.7}O_4$ (x = 0.7) composition with Bragg peak positions, observed, calculated, and difference XRD patterns
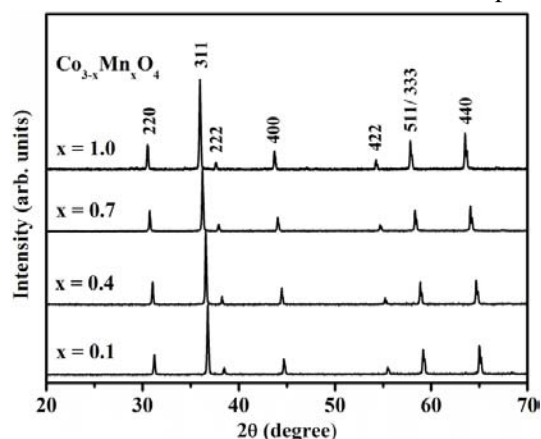
resulting from Rietveld refinement on XRD data. The criteria of the fitting quality on the experimental data were confirmed according to Young[21]. The refined lattice parameter, a, and goodness of fit (GoF), χ^2, are presented in Table 1. An analytical approach also used to calculate 'a' for cubic system through the following equation[22]:

$$\sin^2\theta = (\lambda^2/4a^2)(h^2 + k^2 + l^2) \qquad \ldots(1)$$

where θ is the half of the diffraction angle, λ= 1.54060 Å wavelength of the X-rays, and h, k, l are the Miller indices for diffraction planes as shown in Fig. 1. The linear fit of Eq. (1) is shown in Fig. 3 for polycrystalline CMO (x = 0.1, 0.4, 0.7, and 1.0) ceramic samples. The lattice parameter 'a' can be estimated from the slope of Eq. (1) for the cubic CMO system and are presented in Fig. 4 and Table 1. Figure 4 shows the variation of lattice parameter 'a' for $Co_{3-x}Mn_xO_4$ compositions with varying x, and the inset in the Fig. 4 shows the measured shift in the (311) peak position towards lower angles with increasing Mn content. The estimated value of the lattice constant 'a' through Rietveld refinement and analytical method increases linearly with increasing Mn content in CMO system (Table 1, and Fig. 4), and is found to be in agreement with earlier reported results and the detailed analysis of XRD data was reported elsewhere[14, 19].

Figure 5 shows the variation of dielectric constant, $\varepsilon'(\omega)$, as a function of temperature at different fixed frequencies (100, 300, 500, 700 and 900 kHz) for polycrystalline ceramic $Co_{3-x}Mn_xO_4$ with x = 0.1, 0.4,

Fig. 1—X-ray diffraction patterns for the polycrystalline ceramic compositions $Co_{3-x}Mn_xO_4$ (x = 0.1. 0.4, 0.7, and 1.0) recorded at room temperature.
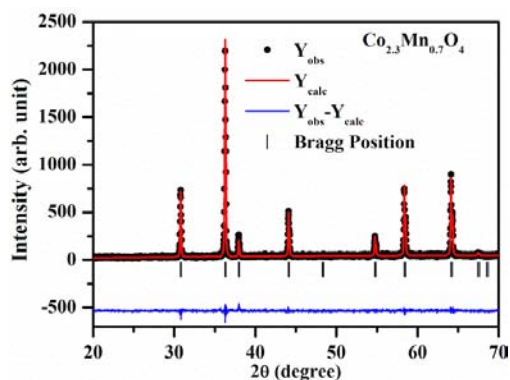

Fig. 2—Rietveld refinement result of XRD data for typical ceramic composition $Co_{0.3}Mn_{0.7}O_4$, experimental pattern (black dots), calculated pattern (continuous red line), and difference them (continuous blue line). Vertical markers (black) indicate the positions of the calculated Bragg reflections

0.7, and 1.0 compositions. The $\varepsilon'(\omega)$ was found to decrease with decreasing temperature and increasing frequency for all CMO ceramic compositions. The $\varepsilon'(\omega)$ shows a weak frequency dispersion and small temperature dependence at lower temperature for all the ceramic compositions. However, at higher temperatures a strong dependence and large frequency dispersion is observed [(Fig. 5 (a)-(d)]. The dielectric

Table 1—Lattice constant (a), goodness of fit (χ^2), dielectric constant (ε'), loss tangent (tanδ) at 300 K, and crossover temperature (T_{CO}) of exponent factor (s) for $Co_{3-x}Mn_xO_4$ compositions

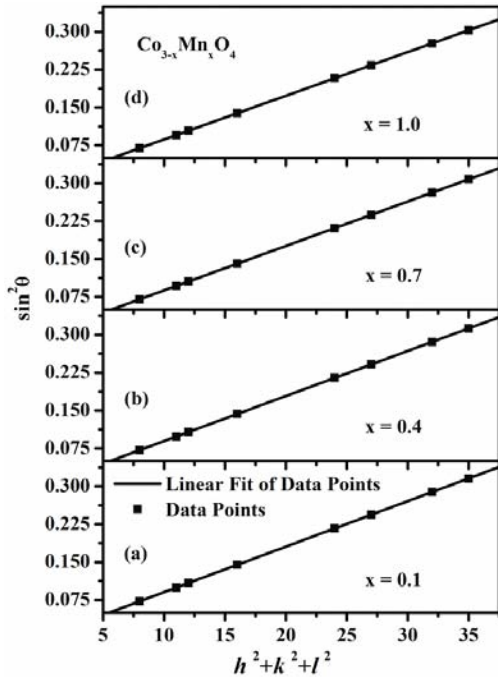| Compositions $Co_{3-x}Mn_xO_4$	Lattice Constant a (Å) R. R. Method	GoF χ^2	ε' (500 kHz)	tanδ (500 kHz)	T_{CO} (K)
$x = 0.1$	8.097(1)	1.12	162	0.05	412
$x = 0.4$	8.145(1)	1.07	322	0.85	300
$x = 0.7$	8.208(1)	1.09	849	0.59	259
$x = 1.0$	8.276(1)	1.19	1759	0.56	258

Fig. 3—Variation of $\sin^2\theta$ versus $h^2 + k^2 + l^2$ for $Co_{3-x}Mn_xO_4$ with (a) $x = 0.1$, (b) $x = 0.4$, (c) $x = 0.7$, and (b) $x = 1.0$ ceramic compositions
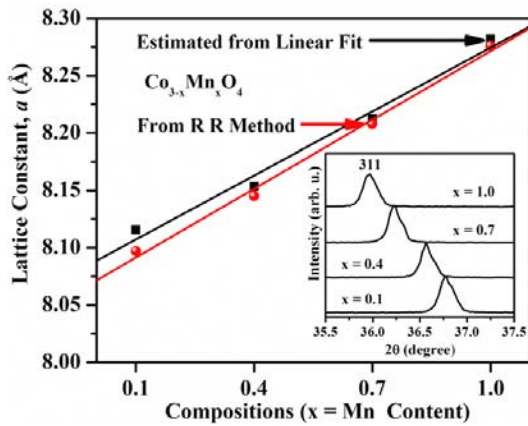

Fig. 4—Variation of lattice parameter (a) and a linear fit of lattice parameter data for the $Co_{3-x}Mn_xO_4$ ($x = 0.1$. 0.4, 0.7, and 1.0) ceramic as a function of compositions (x= Mn content), inset shows the shift in the peak position for 311 reflections
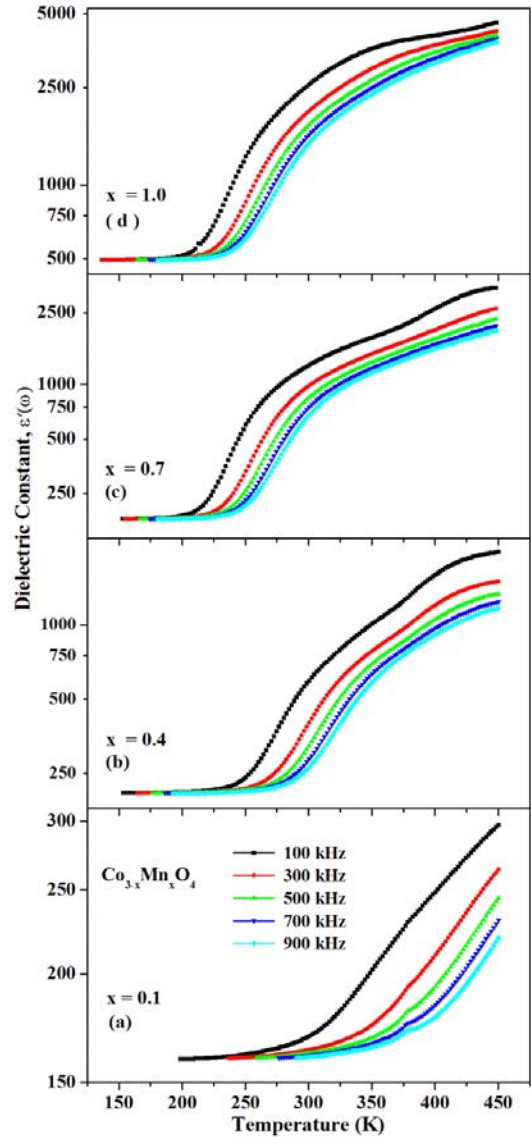

Fig. 5—Variation of dielectric constant, $\varepsilon'(\omega)$, with temperature for $Co_{3-x}Mn_xO_4$ with (a) $x = 0.1$, (b) $x = 0.4$, (c) $x = 0.7$, and (b) $x = 1.0$ ceramic compositions

constant, $\varepsilon'(\omega)$ at each temperature and fixed frequency was found to increase with increasing Mn content in Co_3O_4 (Table 1 and Fig. 5). The observed increase in $\varepsilon'(\omega)$ with Mn content at all measured frequencies and temperature may be attributed to a possible increase in the off centre cubic symmetry in the unit cell of CMO with increasing substitution of Mn (ionic radii of Mn > ionic radii of Co) in Co_3O_4. The presence of the hump in $\varepsilon'(\omega)$ with temperature could be related to the presence of a dielectric anomaly peak. The presence of a such dielectric anomaly peak in $\varepsilon'(\omega)$ was explained in detail in our previous paper[14] and showed room temperature ferroelectricity.

The variation of dielectric loss tangent (tanδ) with temperature at different fixed frequencies (100, 300, 500, 700 and 900 kHz) for as prepared ceramic CMO (x = 0.1, 0.4, 0.7, and 1.0) compositions is shown in Fig. 6. At low temperature (below 175 K), tanδ was found to be almost independent of frequency for all the CMO compositions. However, for a given temperature and composition (x), tanδ was found to decrease with increase in frequency. The low concentration of Mn (x = 0.1) does not show a peak at any frequency in the dielectric loss tangent [inset of Fig. 7(a)]. This might be due to shifting of the peak which is beyond the temperature range in our investigation. The overall higher values of tanδ observed in all Mn substituted Co_3O_4 compositions (Table 1), may be due to an increase in dc conductivity of the materials with Mn substitution. A peak (hump) like structure in tanδ as a function of temperature has been observed at all fixed frequencies for Mn substituted Co_3O_4 compositions [insets of Figs. 7 (b-d)]. For all compositions (except x = 0.1), the temperature, at which the hump in tanδ appears, shifts towards higher temperature as frequency increases. The presence of a hump in tanδ were found in the temperature range 200-350 K, at all the measured fixed frequencies and is shown clearly in the insets of Fig. 6 (b-d), and the peak temperature was found to decrease towards lower temperatures with increasing Mn content. This behaviour of dielectric loss tangent, strongly suggests a dielectric relaxation process. The strong frequency dependent dielectric properties are attributed to the interaction among the free charge carriers (electrons or holes) with potential barriers at grain boundaries, resulting in the enhancement of conductivity[23]. It is clear that, both

values of ε' and tanδ decrease with increase in frequency which is the normal dispersion behaviour of semiconducting oxides. This is attributed to the relatively higher conductivity of the materials, due to the existence of space charges and traps.

Capacitance measurements on the CMO ceramic compositions have been carried out in the high frequency range starting from 100 to 900 kHz, greater than the frequencies corresponding to the time constants suggested by the Catalan[24]. This can be ruled out the possibility of contribution from
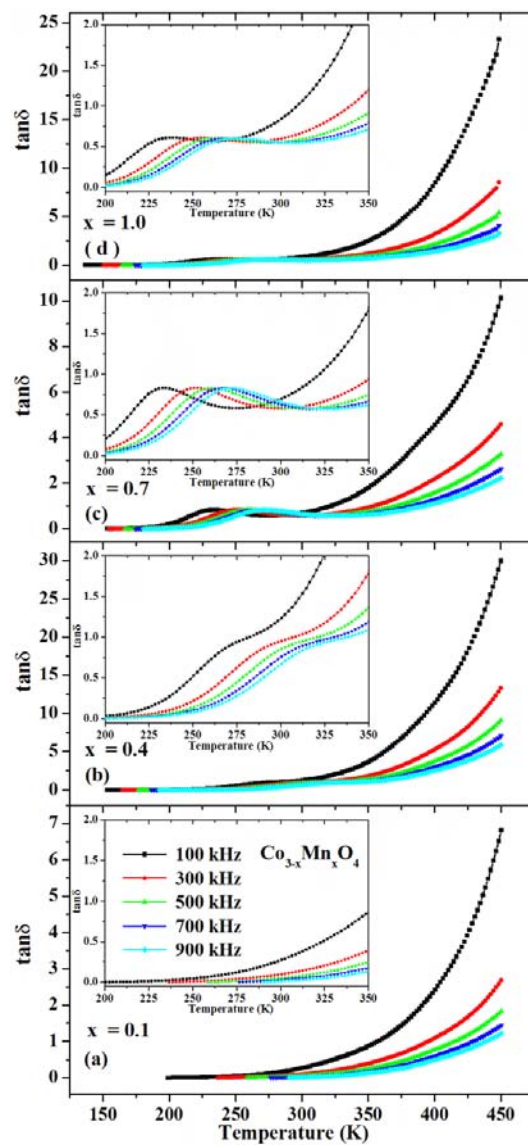

Fig. 6—Variation of dielectric loss tangent, tanδ, with temperature for $Co_{3-x}Mn_xO_4$ with (a) x = 0.1, (b) x = 0.4, (c) x = 0.7, and (b) x = 1.0 ceramic compositions and their corresponding insets show the peaks in tanδ with temperature
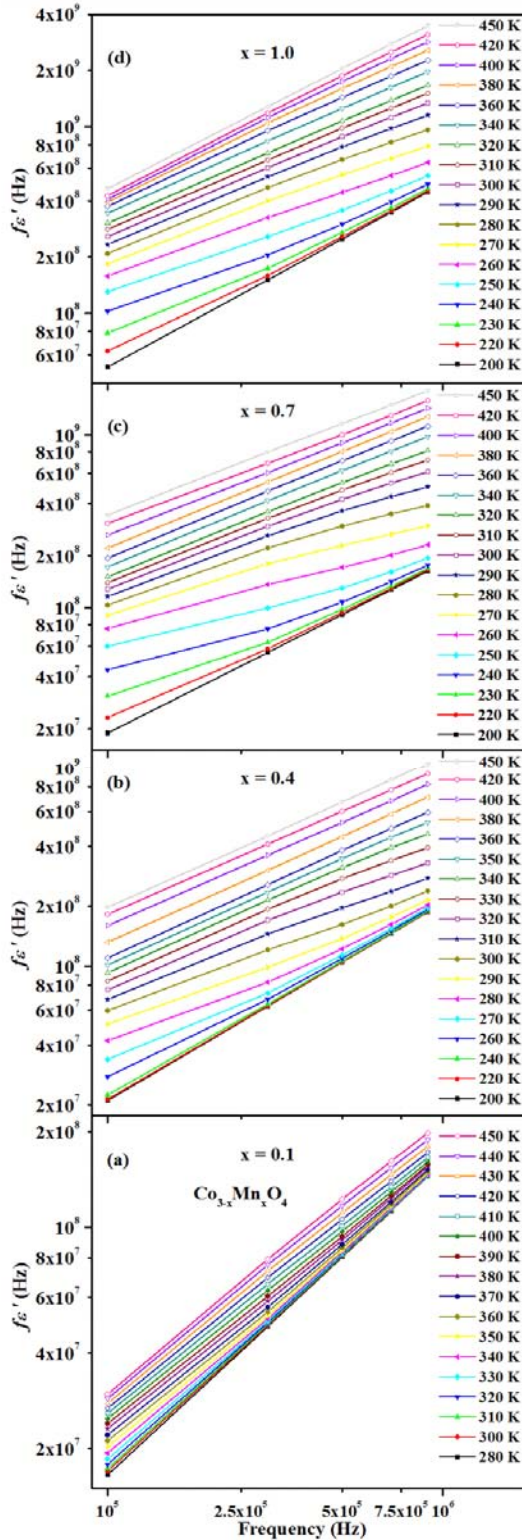
Fig. 7—Variation of log($f\varepsilon'$) versus log(f) for the Co$_{3-x}$Mn$_x$O$_4$ with (a) x = 0.1, (b) x = 0.4, (c) x = 0.7, and (b) x = 1.0 ceramic compositions at fixed different temperatures

Maxwell-Wagner interfacial polarization at low frequencies to the capacitance. At high frequencies, most of the systems exhibit the intrinsic capacitance and need not be an artifact effect. Wang *et al*[25]. observed two types of capacitive contribution above 100 K in TbMnO$_3$ system by grain boundary effect i.e. internal layer barrier capacitor (IBLC) and grains i.e. hopping of charge carriers within the grain (dipolar effect) and the TbMnO$_3$ system followed the universal dielectric response (UDR). It is important to note that the exponentially increasing background at higher temperature in $\varepsilon''(\omega)$ versus temperature (not shown here) or loss tangent, tanδ = ε''/ ε', versus temperature [Fig. 7 (a-d)] at different fixed frequencies suggests that the background is associated with the hopping conductivity (tan$\delta \sim \sigma_{ac}/\varepsilon'\omega \sim$ exp $(-\Delta E/k_BT)/\varepsilon'\omega$, where ΔE is the activation energy of the conductivity and $\omega = 2\pi f$ is the angular frequency). This behaviour of tanδ strongly recommends that the observed relaxation might be correlated to the hopping conductivity. In fact, localized charge carriers hopping between spatially fluctuating lattice potentials not only produce the conductivity but also give rise to dipolar effects. Correlated with these two aspects is the universal dielectric response (UDR) and the dielectric constant, ε', for wide frequency range which can be calculated as[26]:

$$f\varepsilon' = \tan(s\pi/2)\sigma_0 / \varepsilon_0 f^s \qquad \qquad \ldots(2)$$

where σ_0 and s are temperature dependent constants and ε_0 is the dielectric constant of free space. For UDR behaviour, if it is true, at a particular given temperature a straight line with the slope of s should be obtained in the plot of log($f\varepsilon'$) versus log(f). This implication was well confirmed on the log-log graph in Fig. 7(a-d) for Co$_{3-x}$Mn$_x$O$_4$ (x = 0.1, 0.4, 0.7, and 1.0) compositions at different fixed temperature and frequency in the range 100-900 kHz.

It is clear from Fig. 7, the exact straight line behaviour for low Mn content sample i.e. x = 0.1 is observed at all temperatures whereas slight deviation from exact straight line for higher Mn content samples. We note that good straight lines can be obtained at the highest temperatures for all CMO compositions. For $x > 0.1$ with decreasing temperature, the localized carriers are becoming frozen, which reduces the dipolar effects, resulting in the gradual deviation from the straight line. At the same time, the freezing process leads to a large
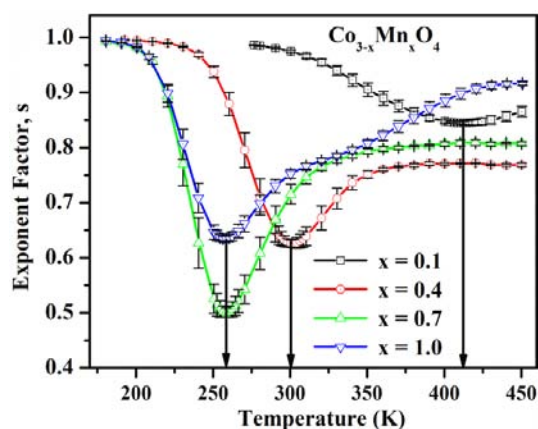
Fig. 8—Variation of exponent factor, s, with temperature for the $Co_{3-x}Mn_xO_4$ (x = 0.1, 0.4, 0.7, and 1.0) ceramic compositions

reduction in number of the hopping carriers, which greatly increases the resistance. The frozen carriers no longer have contributions to the polarization, and the observed dielectric behaviour is dominated by the remaining charge carriers. These carriers still obey the UDR law. Therefore, as the freezing process moves out of the measuring frequency range at low temperatures the linear behaviour of $\log(f\varepsilon')$ versus $\log(f)$ appears again as clearly seen from Fig. 7.

The UDR exponent factor, s, were estimated from the $\log(f\varepsilon')$ versus $\log(f)$ plot (Fig. 7) in the temperature range 175-450 K and shown in Fig. 8 for CMO ceramic with x = 0.1, 0.4, 0.7, and 1.0 compositions. At low temperature the exponent factor 's' shows a very weak dependency on temperature and close to unity for all prepared ceramic compositions. The values of s decrease as temperature increases and attain a lowest value at 412 K (for x = 0.1), 300 K (for x = 0.4), and 259 K (for x = 0.7 and x = 1.0) temperatures,and then increase (Fig. 8 and Table 1). The lowest value of s shifted towards lower temperature for substitution of Mn ions up to $x < 0.7$ and for higher Mn ($x \geq 0.7$) content the lowest value of s is at same temperature in CMO ceramics (Table 1). Since $s = 1$ means energy loss per cycle is constant and shows a nearly constant loss behaviour at low temperature (< 200 K)such type of behaviour has been found in many materials[27-33]. This type of behaviour represents the involvement of dielectric relaxation due to localised ionic motions rather than hopping process at low temperatures[33]. In the UDR theory Nowick *et al*[34.] in Y^{3+} and Gd^{3+} doped CeO_2 ceramic compositions the exponent s is predicted to be temperature dependent, and in low temperature

region $s \to 1.0$ as $T \to 0$ as a linear function of temperature, which we have observed. However, at higher temperature the UDR behaviour is prominent for CMO ceramic compositions ($x > 0.1$) and the exponent factor 's' is consistent with Jonscher's assumption[26,35].

5 Conclusions

In summary, the detailed investigations and discussion on the structural and dielectric properties of cobalt based cubic spinel CMO ceramic compositions, have been presented. Single phase polycrystalline bulk ceramic of $Co_{3-x}Mn_xO_4$ (x = 0.1, 0.4, 0.7, and 1.0) compositions by standard solid state reaction technique has been synthesized successfully. The effect on unit cell parameter 'a' with Mn substitution in Co_3O_4 has been characterized by XRD data using Rietveld refinement and analytical method and found to increase as Mn increases.

The temperature dependent dielectric constant, ε', and loss tangent, $\tan\delta$, show a hump like transitionat all measured fixed frequencies and shift from higher temperature to lower temperature with Mn incorporation. The presence of such a feature in ε' with temperature may be due to structural transformation and formation of electrical dipoles and their ordering, showing the ferroelectric nature. The substitution of Mn^{3+} in Co_3O_4 is probably creating off centre symmetry in the unit cell and exhibits the ferroelectric like signature at room temperature. The presence of such behaviour in $\tan\delta$ was linked with dielectric relaxation and also shifts towards lower temperature with Mn incorporation. The temperature relaxation was attributed due to internal layer barrier capacitor by grain boundary and hopping of charge carriers within the grain and the CMO system followed the UDR model. At low temperature, UDR exponent factor($s\to 1.0$ as $T \to 0$) is apparently independent of temperature and composition and at higher temperature falls in Jonscher's assumption.

References

1 AricoA S, Bruce P, Scrosati B, Tarascon J M & Schalkwijk W V, *Nat Mater*, 4(5) (2005) 366.
2 NamK T, Kim D W, Yoo P J, Chiang C Y, Meethong N, Hammond P T, Chiang Y M & Belcher A M, *Science*, 312 (2006) 885.

3   Lou X W, Deng D, Lee J Y, Feng J & Archer L A, *Adv Mater,* 20 (2008) 258.

4   Li Y, Tan B & Wu Y, *Nano Lett*, 8(1) (2008) 265.

5   Xie X, Li Y, Liu Z Q, Haruta M & Shen W, *Nature*, 458 (2009) 746.

6   Jiao F & Frei H, *Angew Chem Int Ed*, 48 (2009) 1841.

7   Dormann J L & Nogues M, *J Phys: Condens Matter*, 2 (1990) 1223.

8   Philip J& Kutty T R N, *Mater Lett*, 39 (1999) 311.

9   Rios E, Pena O, Guizouarn T&Gautier J L, *Phys Status Solidi C*, 1 (2004) S108.

10 Tian Z Y, Ngamou P H T, Vannier V, Kohse-Hoinghaus K & Bahlawane N, *Appl Catalysis B: Environmental*, 117-118 (2012) 125.

11 Wickham D G & Croft W J, *J Phys Chem Solids*, 7 (1958) 351.

12 Aoki I, *J Phys Soc Jpn*, 17 (1962) 53.

13 Eerenstein W, Mathur N D & Scott J F, *Nature (London)*, 442 (2006) 759.

14 Meena P L, Kumar R, Prajapat C L, Sreenivas K& Gupta V, *J Appl Phys*,106 (2009) 024105.

15 Zeng R, Wang J Q, Chen Z X, Li W X & Dou S X, *J Appl Phys*, 109 (2011) 07B520.

16 Zeng R, Wang J Q, Du G D, Li W X, Chen Z X, Li S, Guo Z P& Dou S X,*arXiv:1207.3216 [cond-mat.mtrl-sci]*.

17 Suzuki T, Adachi K & Katsufuji T,*J Magn Magn Mater*, 310 (2007) 780.

18 Yamasaki Y, Miyasaka S, Kaneko Y, He J P, Arima T & Tokura Y, *Phys Rev Lett*, 969 (2006) 207204.

19 Meena P L, Kumar R & Sreenivas K, *Int J Phys Chem & Math Sci*, 3(1) (2014) 7.

20 Rios E, Lara P, Serafint D, Restovic A&Gautier J L, *J Chil Chem Soc*, 55 (2010) 261.

21 Young R A,*The Rietveld Method* (International Union of Crystallography, Oxford University Press, 1993) 21.

22 Suryanarayana C & Norton M G, *X-ray Diffraction A: Practical Approach* (Plenum Press New York & London, 1998) 102.

23 Maier J, Prill S & Reichert B, *Solid State Ionics*, 28-30 (1988) 1465.

24 Catalan G,*App Phys Lett*, 88 (2006) 102902.

25 Wang C C, Cui Y M & Zhang L W, *App Phys Lett*, 90 (2007) 012904.

26 Jonscher A K, *Dielectric Relaxation in Solids* (Chelsea Dielectrics Press Limited, London, 1983).

27 Wong J& Angell C A,*Glass: Structure by Spectroscopy*, (Marcel Dekker, New York, 1976) 750.

28 LongA R, *Adv Phys*, 31 (1982) 553.

29 Lee W K, Liu J F &Nowick A S, *Phys Rev Lett*, 67 (1991) 1559.

30 Lim B S, Vaysleyb A V &Nowick A S, *Appl Phys A: Solids Surf A*, 56 (1993) 8.

31 Elliott S R, *Adv Phys*, 36 (1987) 135; *Solid State Ionics*, 70/71 (1994) 27.

32 Lu X & Jain H, *J Phys Chem Solids*, 55 (1994) 1433.

33 Sidebottom D L, Green P F & Brow R K, *J Non-Cryst Solids*, 203 (1996) 300.

34 Nowick A S, Vaysleyb A V & Kuskovsky I, *Phy Rev B*, 58 (1998) 8398.

35 Jonscher A K, *Nature (London)*, 267 (1977) 673.